Perilipin-2-null mice are protected against diet-induced obesity, adipose inflammation, and fatty liver disease[S]

James L. McManaman,[1,2,*,†] Elise S. Bales,[*] David J. Orlicky,[**] Matthew Jackman,[†,††] Paul S. MacLean,[†,††] Shannon Cain,[†] Amanda E. Crunk,[§] Ayla Mansur,[§§] Christine E. Graham,[§§] Thomas A. Bowman,[§§] and Andrew S. Greenberg[1,2,,§§]

Division of Basic Reproductive Sciences,* the Center for Human Nutrition,† Graduate Program in Molecular Biology,§ Department of Pathology,** Division of Endocrinology and Metabolism,†† University of Colorado School of Medicine, Aurora, CO; and the Jean Mayer United States Department of Agriculture Human Nutrition Research Center on Aging, Tufts University, Boston, MA§§

Abstract The cytoplasmic lipid droplet (CLD) protein perilipin-2 (Plin2) is expressed in multiple nonadipose tissues, where it is thought to play a role in regulating their lipid storage properties. However, the extent to which Plin2 functions in nutrient utilization and metabolism, or how it influences the consequences of over-feeding, remains unclear. In this study, we demonstrate that the absence of Plin2 prevents high-fat diet(HFD)-induced obesity in male and female mice. This response is associated with increased formation of subcutaneous beige adipocyte cells with uncoupling protein 1 expression, and amelioration of inflammatory foci formation in white adipose tissue and steatosis in the liver. Experiments demonstrate that Plin2 loss results in reduced energy intake and increased physical activity in response to HFD feeding. Our study provides the first evidence that Plin2 contributes to HFD-induced obesity by modulating food intake, and that its absence prevents obesity-associated adipose tissue inflammatory foci and liver steatosis.—McManaman, J. L., E. S. Bales, D. J. Orlicky, M. Jackman, P. S. MacLean, S. Cain, A. E. Crunk, A. Mansur, C. E. Graham, T. A. Bowman, and A. S. Greenberg. **Perilipin-2-null mice are protected against diet-induced obesity, adipose inflammation, and fatty liver disease.** ***J. Lipid Res.*** **2013.** 54: **1346–1359.**

Supplementary key words food consumption • metabolism • gene expression • activity

Obesity, resulting from increased calorie consumption and decreased energy expenditure, remains a major public health concern for children and adults in the United States (1), through its strong etiological links to several metabolic complications, including metabolic syndrome, type 2 diabetes, and nonalcoholic fatty liver disease (NAFLD) (2). Obesity-associated NAFLD in particular is associated with development of hyperlipidemia, insulin resistance, hyperglycemia (3), and increased risk of liver cancer (4, 5). In tissues, neutral lipids such as triacylglycerol are stored in cytoplasmic lipid droplets (CLDs), which are specialized organelle-like structures that function in intracellular trafficking and metabolism of lipids (6). Alterations in CLD properties are increasingly recognized to be associated with metabolic abnormalities and disruptions of normal cellular and tissue functions (7).

Perilipins (PLINs) are a family of genes encoding five CLD-associated proteins in mammals that are implicated in the regulation of storage and hydrolysis of neutral lipids (7, 8). Prior studies investigating reduced expression of perilipin1 (Plin1) in mice demonstrated that it is required for normal adipose lipid storage (9–11), whereas reduced perilipin-2 (Plin2) expression prevents hepatic lipid accumulation in response to high-fat diet (HFD) feeding (12–14). Although Plin1-null mice are also resistant to obesity and many of its attendant metabolic abnormalities (9, 10), there is limited understanding of the contributions of Plin2, or other PLIN family members, to obesity or other metabolic disorders.

Defining the roles of Plin2 in obesity and metabolism has been complicated by observations that existing Plin2-deficient mice produce a truncated product that is biologically active (15), and that the short-term-diet models used previously did not adequately investigate Plin2 regulation

This research was supported by National Institutes of Health Grants 2RO1HD-045962 (J.L.M.), RO1DK-038088 (P.S.M.), F32DK-095538 (T.A.B.), and RO1DK-082574 (A.S.G.), the U.S. Department of Agriculture, Agricultural Research Service, under agreement no. 58-1950-7-70, and the Colorado Nutrition and Obesity Research Center (NORC, DK-48520).

Manuscript received 18 December 2012 and in revised form 1 February 2013.

Published, JLR Papers in Press, February 12, 2013
DOI 10.1194/jlr.M035063

Abbreviations: CLD, cytoplasmic lipid droplet; CLS, crown-like structure; H and E, hematoxylin and eosin; HF, high fat; HFD, high-fat diet; NAFLD, nonalcoholic fatty liver disease; PLIN, perilipin; PPARα, peroxisome proliferator-activated receptor α; qRT-PCR, quantitative real-time PCR; RER, respiratory exchange ratio; WT, wild-type.

[1] Co-senior author.
[2] To whom correspondence should be addressed.
e-mail: jim.mcmanaman@ucdenver.edu (J.L.M.); andrew.greenberg@tufts.edu (A.S.G.).

[S] The online version of this article (available at http://www.jlr.org) contains supplementary data in the form of one figure.

of body fat accumulation (12, 13). To explore the functional importance of Plin2 in obesity and other aspects of lipid metabolism, we generated a new conditional line of mice in which the Plin2 locus was disrupted by targeted removal of exon 5. In this paper, we document that mice lacking Plin2 are resistant to HFD-induced obesity. Our studies further show that Plin2 loss prevents HFD-induced obesity largely by limiting energy intake and altering locomotor activity.

METHODS

Materials

Chemicals used were purchased from Sigma Chemical Co. (St. Louis, MO). Antibodies to N- and C-terminal regions of Plin2 and to Plin3 were raised in rabbits as described (15). Guinea pig antibodies to mouse Plin1, Plin4, and Plin5 were purchased from Fitzgerald (North Acton, MA). Antibodies to mouse F4/80 were purchased from Serotec (Raleigh, NC). HRP-conjugated and Alexfluor-conjugated secondary antibodies were purchased from Life Technologies (Grand Island, NY). HF (60 kcal%; D12492) and low-fat (10 kcal%, D12045B) diets were purchased from Research Diets, Inc. (New Brunswick, NJ).

Generation of Plin2(Δ5) mice

Mice lacking exon 5 of the Plin2 locus were generated using a targeting strategy that deleted 1.8 kb of the genomic sequence containing the murine Plin2 exon 5, resulting in out-of-frame splicing between exons 4 and 6 (**Fig. 1**). A Flip recombinase target site (FRT)-neomycin-FRT-*lox*P cassette and a distal *lox*P site were inserted into introns 4 and 5, respectively, of a mouse genomic DNA encompassing Plin2 gene regions surrounding exon 5 that was cloned from a 129Sv/Pas miniBAC library (genOway; Lyon, France) and that is isogenic to the ES cell line used for homologous recombination. Short- and long-homology arms were generated using the following sets of primer pair sequences: Short-homology arm, forward, CGTGGGTAGCTTTATTTCCTGAGTGACG, and reverse, CATAGGTATTGGCAACCGCAACTGC, amplify a 345 bp segment in intron 3 and exon 4 of Plin2. Long-homology arm, forward, TGGTGCATAGTACCTGCCTTCAAATGG, and reverse, TGGTGCATAGTACCTGCCTTCAAATGG, amplify a 549 bp segment in intron 7 of murine Plin2. 129/SvPas ES cells, containing an agouti coat color marker, were transfected with the linearized targeting vector and selected in G418-containing media. Homologous recombinations were identified by PCR and Southern blotting. Targeted ES clones were injected into C57BL/6 blastocysts. Recombinant animals, identified by coat color and PCR genotyping, were crossed with C57BL/6-expressing Cre-recombinase-expressing mice (CMV-Cre, genOway), and offspring were genotyped by PCR to identify those that were heterozygous for the knockout genotype. The knockout genotype of PCR-positive animals was confirmed by Southern blot analysis. Heterozygous knockout animals were backcrossed to C57BL/6 mice for 15 generations to generate congenic C57Bl/6-Plin2(Δ5) mice. Wild-type (WT) and Plin2(Δ5) mice were genotyped by PCR using the following mixture of primer sequences that target exon 5 and adjacent intronic regions of the mouse Plin2 locus: 5′- AGC AAC CTG ATG GAG ACA CTC AG -3′(forward); 5′- CAC TGT TCA TGA ACT GCA CCA TC -3′(reverse 1); 5′- CCG AGA GCA GAG CTT GGT AGA -3′(reverse 2).

Animal housing and dietary treatments

Mice were housed in the University of Colorado School of Medicine's Center for Comparative Medicine at ambient temperatures of 22–24°C on a 12:12 h light-dark cycle with free access to food and water for the study's duration. All mice were fed standard mouse chow ad libitum from weaning to 8 weeks of age, at which time they were placed on isocaloric diets containing 60% fat calories (D12492) or 10% fat calories (D12450B) from Research Diets, Inc. Body weights were measured at weekly cage changes. Upon completion of the feeding experiments, determination of the body composition of each animal was performed by quantitative magnetic resonance EchoMRI-900 whole-body composition analyzer (Echo Medical Systems; Houston, TX), and blood samples were taken for serum analysis. For fasting-feeding experiments, male mice were fasted for 24 h then refed with the 60% fat calorie diet for 16 h. At the termination of each experiment, mice were injected with sodium pentobarbital to induce anesthesia and euthanized by exsanguination. After euthanization, organs and tissues were removed from each animal, weighed, and processed for histological, immunohistochemical, and biochemical analyses. The University of Colorado School of Medicine Institutional Animal Care and Use Committee approved all procedures.

Metabolic monitoring

Three separate cohorts of mice were placed in a metabolic monitoring system that provided measurements of energy balance (intake and expenditure), the respiratory exchange ratio (RER), and activity levels (Columbus, OH; 8M Oxymax) (16). Mice were individually housed in metabolic chambers after 9 weeks of HF feeding. Metabolic measurements were made following a 3 day lead-in to allow the mice to adjust to the chambers.

Histology and immunohistochemistry

Freshly dissected organ and tissue sections were processed for hematoxylin-and-eosin (H and E) staining and immunofluorescence microscopy as described previously (17). Immunoreactivity was visualized using secondary antibodies conjugated with Alexafluor 488 or Alexafluor 594 at dilutions of 1:500 and 1:250, respectively. Nuclei were stained with (4′,6-diamidino-2-phenylindole (Sigma Chemical Co.). Immunofluorescence images were captured on a Nikon Diaphot fluorescence microscope and digitally deconvolved using the No Neighbors algorithm (Slidebook; Denver, CO) as described previously (17). Histologic images were captured on an Olympus BX51 microscope equipped with a four megapixel Macrofire digital camera (Optronics; Goleta, CA) using the PictureFrame Application 2.3 (Optronics). All images were cropped and assembled using Photoshop CS2 (Adobe Systems, Inc.; Mountain View, CA).

RNA extraction and transcript quantitation

Total RNA was extracted and its purity and integrity quantified as described previously (15). PLIN family transcript copy numbers were determined by quantitative real-time PCR (qRT-PCR) analysis by the Quantitative Genomics Core Laboratory at the University of Texas Health Sciences Center using a multiplexing strategy, with validated primer-probe sets and 18S rRNA as a standard (15). The primers and probes used for qRT-PCR analyses are listed in Table 1 in the supplementary data. Three tissue replicates at each time point were analyzed.

Protein extraction and analyses

Liver samples were homogenized on ice with glass-on-glass grinding tubes in homogenization buffer (20 mM Tris-HCl, pH 7.4; 150 mM NaCl; 1% NP-40; 20 mM NaF; 2 mM EDTA, pH 8.0; 2.5 mM NaPP; 20 mM β-glycerophosphate; 1% glycerol; ddH_2O) plus protease and phosphatase inhibitors (aprotinin, leupeptin, pepstatin, AEBSF, PIC1, PIC2). Protein concentration

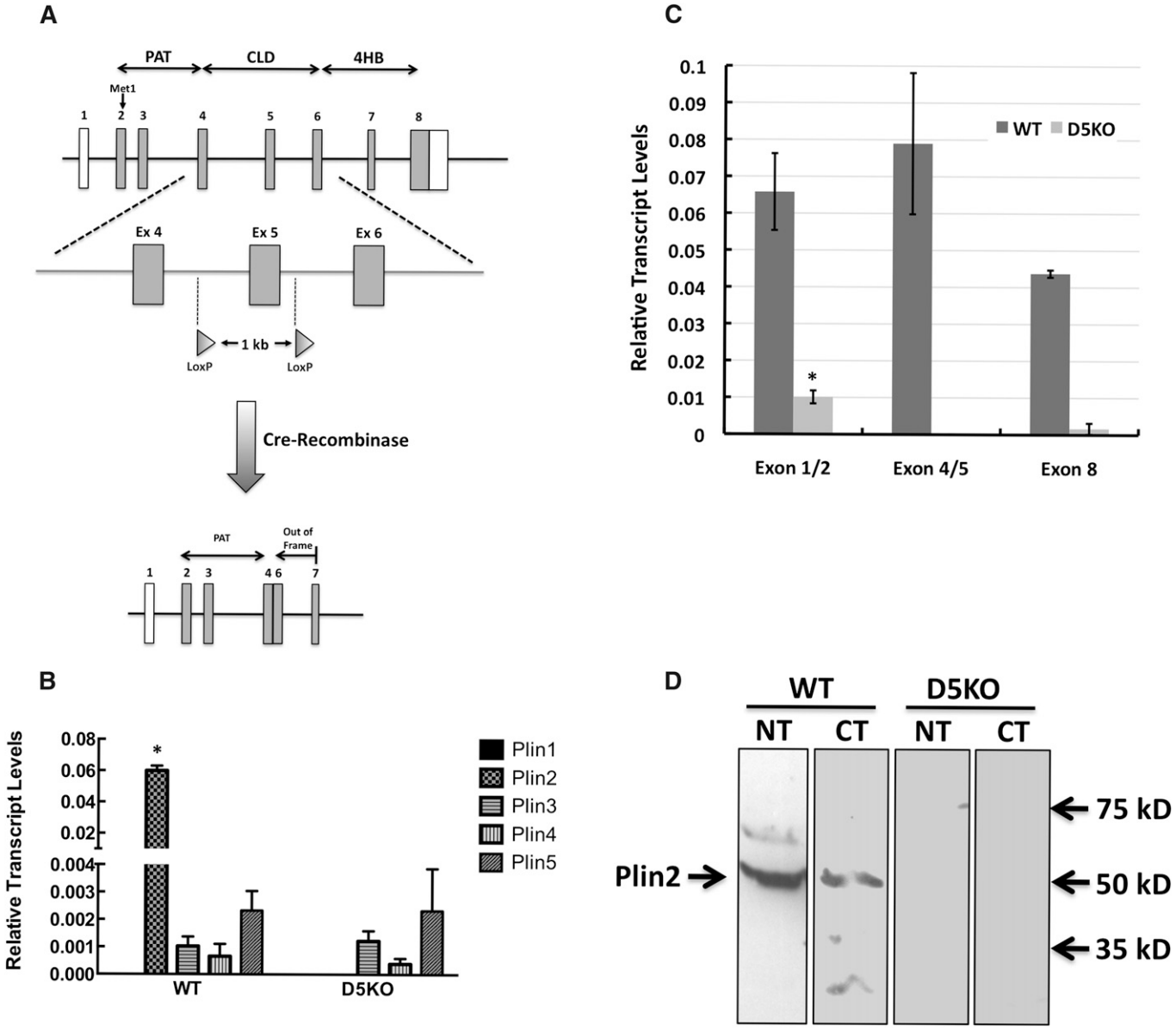

Fig. 1. Generation of Plin2(Δ5) mice. A: Scheme used for disrupting the Plin2 locus. Transgenic mice harboring *lox*P sites flanking exon 5 of the Plin2 locus were crossed with Cre-recombinase-expressing mice to produce mice in which exons 4 and 6 in the Plin2 locus are fused, generating a frame-shift mutation and a premature stop codon in exon 7. B: Transcript levels of PLIN family members in livers of fasted and refed WT and Plin2(Δ5) mice (referred to as D5KO in all figures). Values are means ± SD normalized to 18S RNA. C: Exon 5 excision does not generate alternate splice forms of Plin2. The relative levels of exon 1–2, exon 4–5, and exon 8 products in fasted and refed livers of WT and Plin2(Δ5) mice were quantified by qRT-PCR and are shown as means ± SD normalized to 18S RNA. D: Plin2 is not detectable in livers of Plin2(Δ5) mice. Representative immunoblots of liver extracts (50 μg) from fasted and refed WT and Plin2(Δ5) mice probed with antibodies to N-terminal (NT)- and C-terminal (CT)-specific sequences of mouse Plin2 (15). Bands corresponding to full-length Plin2 in liver extracts from WT mice and the relative positions of selected molecular weight standards are indicated with arrows. Statistically significant differences are indicated by asterisks

was measured using the DC Protein Assay Kit II (Bio-Rad Laboratories; Hercules, CA). Fifty microgram amounts of total protein were separated on 7.5% SDS-polyacrylamide gels, transferred to a 0.2 μm nitrocellulose membrane, and probed with the 1/1,000 dilutions of rabbit antibodies to the N- and C-terminal regions of Plin2 (17). Corresponding HRP-conjugated secondary antibodies were used at 1/5,000 dilution. Bands were detected using SuperSignal West Pico chemiluminescent substrate (Thermo Fisher Scientific, Inc.; Rockford, IL), and band intensities were quantified by densitometry using the ChemiDoc system (Bio-Rad Laboratories).

Statistical analysis

Data were analyzed by Students *t*-test. Statistical significance was assumed when $P \leq 0.05$.

RESULTS

Targeted disruption of exon 5 in the mouse Plin2 locus leads to loss of Plin2 expression

We generated Plin2(Δ5) mice by crossing transgenic mice harboring *lox*P sites flanking exon 5 of the Plin2

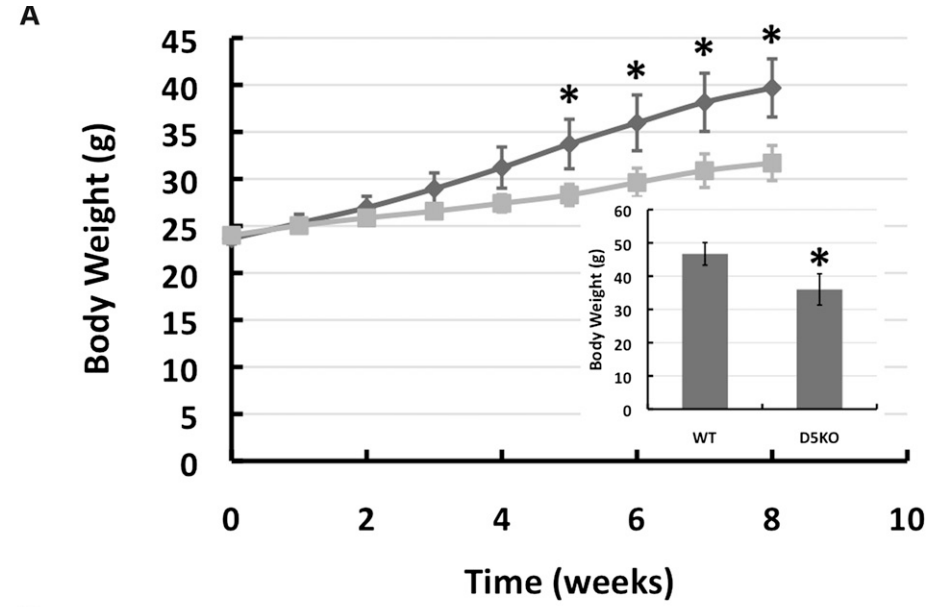
A
Body Weight (g)
Time (weeks)
Body Weight (g)
WT
D5KO

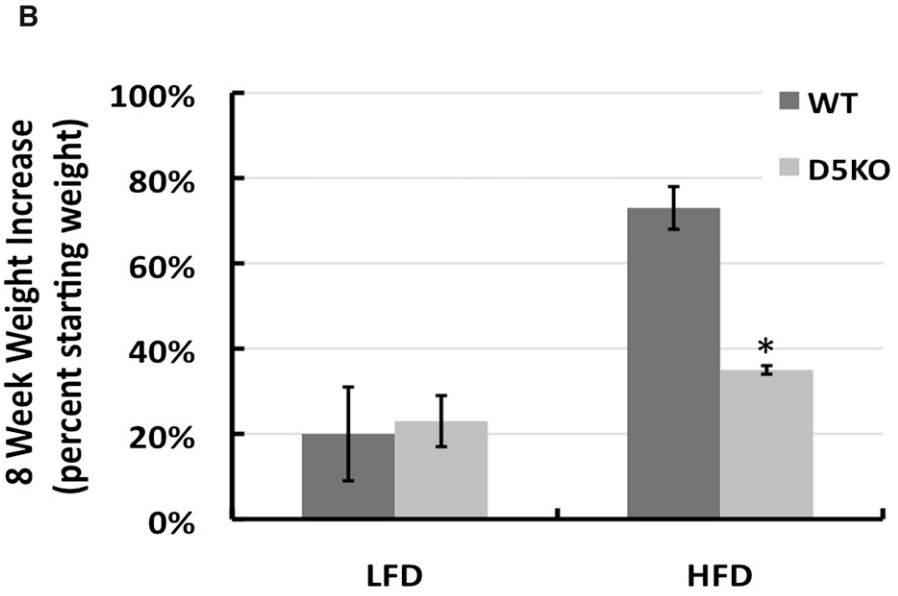
B
8 Week Weight Increase
(percent starting weight)
WT
D5KO
LFD
HFD

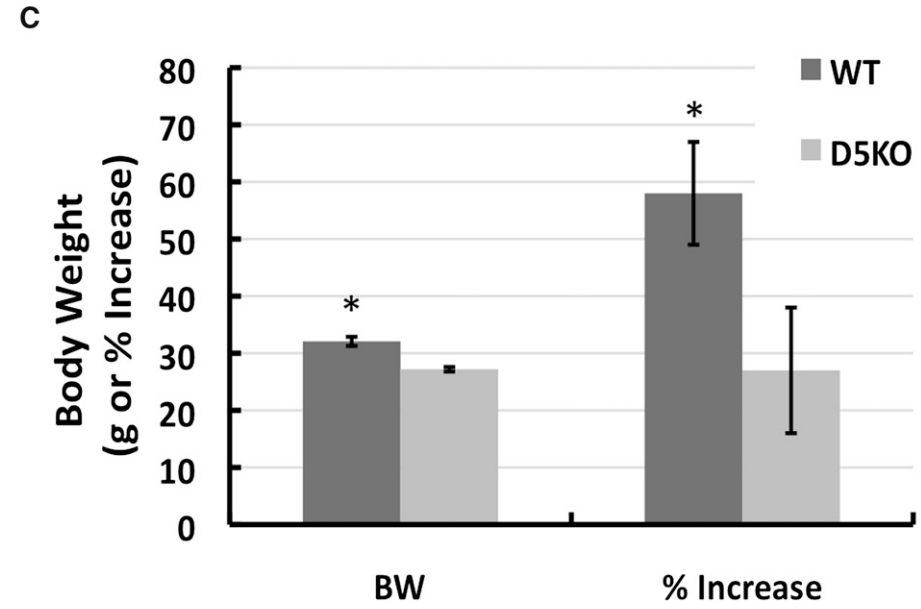
C
Body Weight
(g or % Increase)
WT
D5KO
BW
% Increase

locus with C57BL/6 mice globally expressing Cre-recombinase, including in the germ line (Fig. 1A). Subsequently, the Cre gene was removed by mating, yielding mice expressing a mutated Plin2 locus under control of the CMV promoter in the absence of Cre expression. Mutant Plin2(Δ5) mice on a mixed C57BL/6-129 background were then backcrossed with C57BL/6 males for over 15 generations. Congenic C57BL/6 mice lacking the Plin2 gene were identified by PCR analysis (see supplementary Fig. I). Primer sequences targeted to exon 5 and adjacent intronic regions (see Methods) amplified a 387 bp band in WT mice and a 300 bp band in Plin2(Δ5) mice. Excision of exon 5 was predicted to produce a truncated transcript in which exons 4 and 6 are fused, generating a frame-shift mutation and a premature stop codon in exon 7 that we hypothesized would result in degradation of the Plin2 mRNA (Fig. 1A).

We investigated whether exon 5 deletion disrupts Plin2 expression by determining Plin2 transcript and protein levels in livers of WT and Plin2(Δ5) mice that had been fasted and then refed with a 60% fat diet. A fasting-and-refeeding protocol has previously been demonstrated to significantly increase hepatic Plin2 mRNA and protein expression (18). Studies using qRT-PCR revealed that Plin2 transcript levels, in livers of WT mice, were at least 30-fold greater than those of other PLIN family members (Fig. 1B), indicating that Plin2 is the most highly expressed PLIN family member in livers from mice. To fully characterize how exon 5 removal affects Plin2 transcript properties, we probed hepatic RNA with primers that included the boundaries of exons 1–2 and exons 4–5, and exon 8. We did not detect exon 4–5 or exon 8 Plin2 transcripts in hepatic RNA from Plin2(Δ5) mice (Fig. 1C), confirming that loss of exon 5 disrupts transcription of downstream exons (Fig. 1A). We were able to detect low levels of Plin2 mRNA at the exon 1–2 junction. However, levels of this product were less than 10% of that obtained from hepatic RNA of WT mice, indicating that loss of exon 5 also impairs upstream exon transcription and/or processing. To determine whether mice harboring the Plin2(Δ5) mutation produce a protein product, we probed liver extracts from fasted and refed WT and Plin2(Δ5) mice with antibodies specific to N-terminal and C-terminal sequences of mouse Plin2 (15). Figure 1D demonstrates that both antibodies detected a band in extracts of WT livers corresponding in size to that of full-length Plin2. However, neither antibody detected bands in liver extracts from Plin2(Δ5) mice, which is consistent with the absence of Plin2 protein expression in these animals. Additionally, the relative mRNA levels of other PLIN family members in Plin2(Δ5) livers were comparable to thosefound in WT livers (Fig. 1B), suggesting that disruption of the Plin2 locus does not induce compensatory changes in expression of other PLIN proteins in livers of fasted and refed mice.

Plin2-deficient mice are resistant to obesity induced by an HF diet

Having established that Plin2(Δ5) mice lack detectable amounts of Plin2, we next investigated the effects of Plin2 loss on body fat accumulation in response to HF diet feeding. Like other Plin2-deficient strains (19), we found that Plin2(Δ5) females had difficulty raising their first litters. We are currently investigating the nature of this defect. However, Plin2(Δ5) mice derived from subsequent pregnancies had normal viability and growth rates, and by 8 weeks of age, when HF feeding was started, their body weights were similar to those of WT mice (**Fig. 2A**).

We examined the effects of a high caloric diet in cohorts of 8 week-old male WT and Plin2(Δ5) mice utilizing a low-fat (LF) diet (10% fat calories) or a HF diet (60% fat calories) for 8 to 12 weeks (Fig. 2). We found that providing mice ad libitum with a LF diet increased the average weights of both WT and Plin2(Δ5) mice by about 20% after 8 weeks (Fig. 2B). These weights were not significantly different from each other ($P = 0.43$), thus demonstrating that Plin2 loss does not affect weight gains on a LF diet. However, on a HF diet, Plin2(Δ5) mice gained significantly less weight than did WT mice over an 8–12 week feeding period (Fig. 2A, B). The body weights of WT mice on the HF diet increased by 16 g after 8 weeks and 22 g after 12 weeks (Fig. 2A, inset), whereas the weights of Plin2(Δ5) mice on the HF diet increased by only 8 g after 8 weeks and only 14 g after 12 weeks. Beginning on week 5 of HF feeding, the body weights of WT mice were significantly ($P < 0.05$) greater than those of Plin2(Δ5) mice. These results suggest that Plin2 loss selectively reduces weight gains associated with HF feeding in male mice. We performed similar studies in female mice and found that although females weighed much less than males, the average body weights and the percent weight gain of Plin2(Δ5) females fed the HF diet were also significantly less ($P < 0.01$) than those of HF-fed WT females (Fig. 2C).

HF diet-induced increases in fat accumulation are prevented by Plin2 loss

To determine whether the decreased weight gain observed in HF-fed Plin2(Δ5) mice was associated with selective reduction of fat mass, we quantified the amounts of

Fig. 2. Plin2 loss prevents HF diet-induced weight gain. A: Weight gain profiles of 8 week-old WT (dark line) and Plin2(Δ5) (light line) male mice fed a HF diet for 8 weeks. (Note that the weight of WT and Plin2(Δ5) animals at 8 weeks of age is virtually identical). Values are average body weights ± SEM of three separate cohorts of WT (N = 15) and Plin2(Δ5) (N = 14) mice. The inset shows the average body weights ± SD for two cohorts of WT (N = 7) and Plin2(Δ5) (N = 8) mice after 12 weeks of HF diet feeding. B: Relative increases in body weights of 8 week-old male WT and Plin2(Δ5) mice fed LF or HF diets for 8 weeks. The values are mean (± SD) percent increase in body weights. WT-HFD (N = 6); WT-LFD (N = 6); Plin2(Δ5)-HFD (N = 6); Plin2(Δ5)-LFD (N = 6). C: Body weights and the percent increase in body weight of 8 week-old female WT and Plin2(Δ5) mice fed the HF diet for 8 weeks. Values are means ± SD of WT (N = 6) and Plin2(Δ5) (N = 6) mice.

lean and fat mass in WT and Plin2(Δ5) mice fed the HF diet for 9 weeks (**Fig. 3A**). Whereas fat mass averages for Plin2(Δ5) mice were 60% ($P < 0.003$) less than those of WT controls, Plin2 loss did not appear to affect lean mass quantities (Fig. 3A). For WT and Plin2(Δ5) males on the HF diet, lean mass values after 9 weeks on the diet were comparable to their starting lean masses (Fig. 3B). In contrast, fat mass values for WT males increased by nearly 275%, whereas fat mass values for Plin2(Δ5) mice increased by only about 40% (Fig. 3B).

We also investigated whether the failure to detect effects on HF diet-induced weight gains and body fat mass in other models of Plin2 deficiency (12, 13) was related to differences in the genetic models used for disrupting Plin2 expression, or to the length of the HF feeding periods. We compared the relative weight gains of 8 week-old male mice fed LF or HF diets for 8 weeks (Fig. 3C). Weight gain of Plin2(Δ2,3) mice had previously been compared with WT mice on a 45% fat diet for only 4 weeks (12). The weights of WT and Plin2(Δ2,3) mice both increased by approximately 20% over their starting values on the LF diet; and at 9 weeks, their weights were not statistically different. In contrast, on the HF diet, the relative weight gains of Plin2(Δ2,3) mice after 9 weeks (30%) were significantly

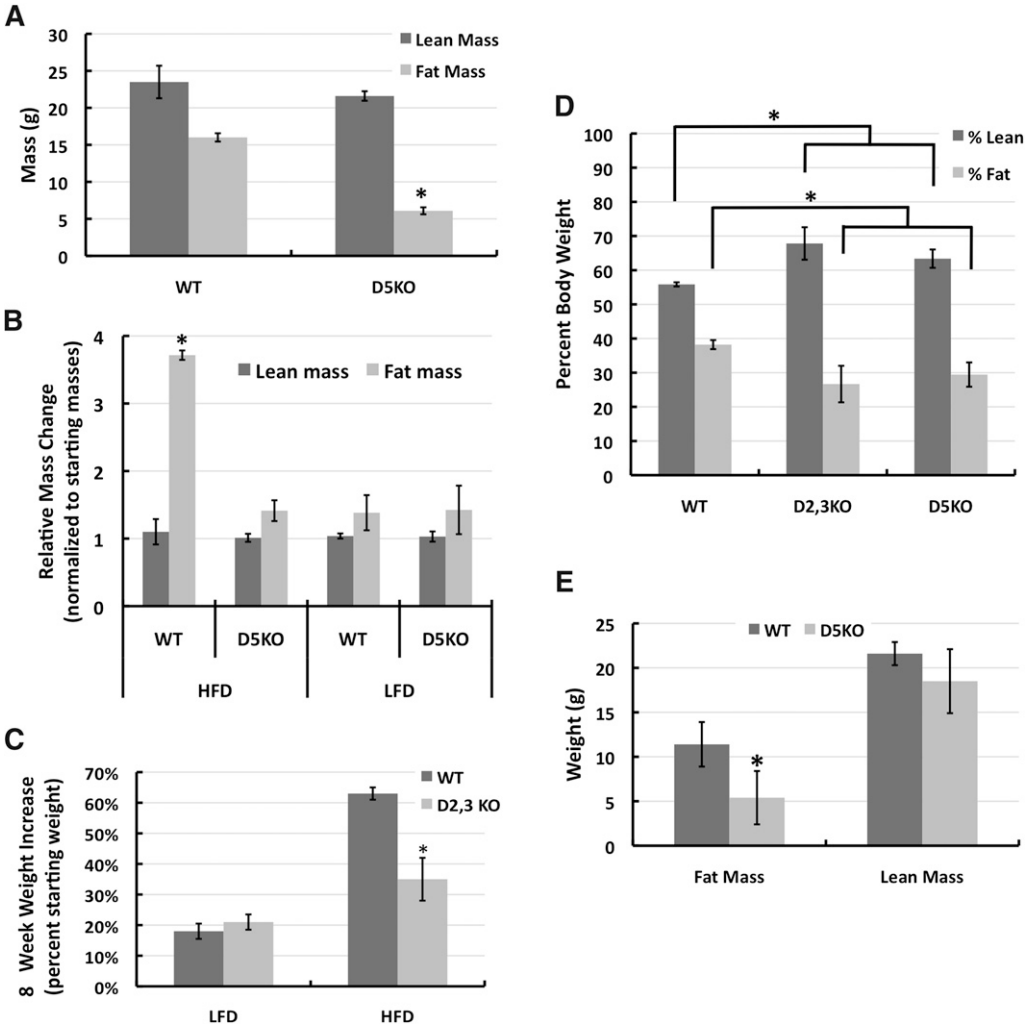

Fig. 3. Plin2 loss reduces adiposity in HF diet-fed mice. A: Body compositions determined by magnetic resonance imaging of male WT and Plin2(Δ5) mice fed the HF diet for 8 weeks beginning at 8 weeks of age. The values are means ± SEM of three separate cohorts of WT (N = 15) and Plin2(Δ5) (N = 14) mice. B: Relative effects of LF and HF diets on body composition of WT and Plin2(Δ5) mice. The values are means ± SD of lean and fat mass weights of 8 week-old male WT and Plin2(Δ5) mice fed LF or HF diets for 8 weeks normalized to their starting weights. WT-HF (N = 15); WT-LF (N = 6); Plin2(Δ5)-HF (N = 14); Plin2(Δ5)-LF (N = 6). C: Relative increases in body weights of 8 week-old male WT and Plin2(Δ2,3) mice fed the HF diet for 9 weeks. The values are average percent increase in body weight ± SD over 8 weeks for WT (N = 6) and Plin2(Δ2,3) (N = 6) mice. D: Effects of HF diet feeding on fat and lean mass composition of WT, Plin2(Δ5), and Plin2(Δ2,3). Eight week-old males from each strain were fed the HF diet for 8 weeks. Lean and fat masses are shown as a percentage of body weight. Values are means ± SD for WT (N = 8), Plin2(Δ5) (N = 8), and Plin2(Δ2,3) (N = 6) animals. E: Effects of 8 weeks of HF feeding, beginning at 8 weeks of age, on mean lean and fat mass weights (± SD) of female WT (N = 6) and Plin2(Δ5) (N = 6) mice. Statistically significant differences are indicated by asterisks.

($P < 0.01$) less than those of WT mice (60%) (Fig. 3C). Similar to HF-fed Plin2(Δ5) mice, Plin2(Δ2,3) mice had significantly lower fat mass values ($P < 0.01$) than their WT counterparts (Fig. 3D) after 9 weeks of feeding, and significantly greater lean mass values ($P < 0.01$). We also found that female Plin2(Δ5) mice were similarly protected against the dramatic increase in fat mass as compared with WT mice (Fig. 3E). Thus, in mice, the effects of Plin2 loss on HF diet gains in adiposity appear to be independent of both gender and genetic models.

Consistent with decreased amounts of body fat, we found that overnight fasting serum leptin levels in HF-fed Plin2(Δ5) mice were about a third of those found in WT mice ($P < 0.04$) (**Table 1**). We also found that fasting levels of serum insulin were lower in Plin2(Δ5) mice compared with WT mice, although the difference did not reach statistical significance ($P = 0.07$) (**Table 2**).

Plin2-null mice on a HF diet have reduced food intake and increased activity levels

To determine whether the resistance of Plin2(Δ5) mice to HF diet-induced weight gains was associated with alterations in energy consumption and/or expenditure, we compared food intake, energy expenditure, and activity levels of male WT and Plin2(Δ5) mice. The weekly food consumption of Plin2(Δ5) mice was less than that of WT mice, reaching significance around week 4 of HF feeding (**Fig. 4A**). In agreement with food consumption measurements, we found that energy intake values, as determined by indirect calorimetry, of male Plin2(Δ5) mice fed the HF diet for 8 weeks were significantly less ($P < 0.01$) than those of WT mice (Fig. 4B), whereas their weight-adjusted energy expenditures were similar to those of WT males (Fig. 4B). The consequence of these differences was that after 8 weeks of HF feeding, WT mice had a positive energy imbalance of about 8 Kcal/day, whereas Plin2(Δ5) mice had a significantly lower ($P < 0.02$) positive energy imbalance of only about 2 Kcal/day. We did not detect differences in the type of fuel utilized for energy by HF-fed Plin2(Δ5) and WT mice as determined by RER, nor did we find differences in the amount of fat in their feces (data not shown). Interestingly, the ambulatory activity of Plin2(Δ5) mice after 8 weeks of HF feeding was significantly greater than that of WT mice (33%, $P < 0.01$, data not shown). Collectively, these data indicate that diminished energy intake and possibly increased activity are the primary contributors to the resistance of Plin2(Δ5) mice to HF diet-induced weight gain.

Plin2 absence reduces adipocyte cell size and inflammatory cell foci and results in appearance of beige adipocytes

Consistent with a decrease in total body fat on a HF diet, we found that after 12 weeks of HF feeding, the epididymal and subcutaneous adipose depot weights of Plin2(Δ5) mice were significantly less than those of WT mice (**Fig. 5A**). Histological analysis revealed that adipocytes in visceral and subcutaneous adipose depots of WT mice were large and contained mainly unilocular fat droplets (Fig. 5B, panels a and b). Epididymal adipose tissue from Plin2(Δ5) mice was also composed of adipocytes with unilocular fat droplets (Fig. 5B, panel c). However, Plin2(Δ5) subcutaneous adipose depots contained extensive areas in which adipocytes possessed multilocular lipid droplets (Fig. 5B, panel d). We immunostained subcutaneous adipose tissue with antibodies to the adipose lipid droplet protein, Plin1, to further establish this observation. Figure 5C demonstrates Plin1 (green staining) localizing to multiple small lipid droplets in subcutaneous adipocytes from Plin2(Δ5) mice. To confirm the effects of Plin2 loss on adipocyte size, we determined the average size of adipocytes in multiple sections from epididymal and subcutaneous adipose tissue from WT and Plin2(Δ5) mice fed the HF diet for 12 weeks. The average diameters of epididymal and subcutaneous adipocytes in HF-fed WT mice were 48 μm and 46 μm, respectively. Loss of Plin2 was associated with a 20% decrease in the relative size of epididymal adipocytes ($P < 0.01$) and a nearly 40% decrease in the relative size of subcutaneous adipocytes ($P < 0.001$) (Fig. 5D).

Plin2 is expressed by adipocytes and localizes to small CLDs during their early differentiation, where it is proposed to contribute to the management of triglyceride (TG) storage during adipose differentiation (20, 21). Consistent with this general notion, the presence of adipocytes with multilocular droplets within subcutaneous adipose tissue of Plin2(Δ5) mice indicates that Plin2 loss may influence development of adipocytes with properties of brown adipocytes, such as UCP1 expression (22). In epididymal

TABLE 1. Serum hormone and lipid levels

	WT	D5KO	*t*-test
Leptin (*ng/ml*)	12.7 ± 3.6	4.7 ± 0.8	$P < 0.05$
Insulin (*ng/ml*)	2.7 ± 0.7	1.1 ± 0.3	$P < 0.07$
Triglycerides (*mg/dl*)	31.5 ± 3.5	24.0 ± 1.4	$P < 0.00005$
FAs (*mM*)	1.2 ± 0.2	0.8 ± 0.2	$P < 0.01$

Fasting serum hormone and lipid levels in WT and Plin2(Δ5) mice fed the HF diet for 12 weeks.

TABLE 2. Liver pathology scores for HF-fed animals

		Pathology score		
WT	0	1	2	3
Macrosteatosis	5	2	0	0
Microsteatosis	1	0	6	0
Fibrosis	6	1	0	0
Microgranulomas	6	1	0	0
Inflammation	7	0	0	0
Ballooning	7	0	0	0
		Pathology score		
D5K0	0	1	2	3
Macrosteatosis	7	0	0	0
Microsteatosis	7	0	0	0
Fibrosis	7	0	0	0
Microgranulomas	7	0	0	0
Inflammation	7	0	0	0
Ballooning	7	0	0	0

Liver pathologies of 12 week HF-fed WT and Plin2(Δ5) mice were evaluated using a modified Kleiner/Brunt scoring system (26) on a scale of 0–3. The numbers indicate the number of animals with a particular pathological score.

adipose tissue of 12 week HF-fed animals, we detected no difference in UCP1 expression between WT and Plin2(Δ5) mice (Fig. 5E). However, in subcutaneous adipose tissue, UCP1 transcript levels in Plin2(Δ5) mice were significantly elevated over WT levels ($P < 0.005$). The mRNA of PGC-1 α, an important coactivator involved in mitochondrial biogenesis (23), also tended to be greater in epididymal adipose tissue of HF-fed Plin2(Δ5) mice compared with WT mice, and greater than the levels found in subcutaneous adipose tissue of WT mice (Fig. 5E). However, the differences did not reach statistical significance ($P = 0.08$). We also found that Plin2 loss was associated with significant increase in the relative expression levels of UCP1 (WT = 1.00 ± 0.22, N = 5; Plin2(Δ5) = 54.23 ± 20.05, N = 5, $P = 0.029$), and PGC-1 α (WT = 1.00 ± 0.06, N = 5; Plin2(Δ5) = 2.55 ± 0.26, N = 5, $P = 0.004$) in subcutaneous adipose tissue of chow-fed mice. In summary, these findings suggest that subcutaneous adipose tissue in our line of Plin2-null mice exhibits properties of brown-like, or beige, adipocytes; and that when on a HF diet, adipocyte size in epididymal and subcutaneous adipose tissue is reduced by the absence of Plin2.

Obesity-associated inflammation has been linked to the development of metabolic complications. A histological hallmark of obesity-associated adipose tissue inflammation is the appearance of crown-like structures (CLSs), which are composed of macrophages localized around, and scavenging, the lipid remnants of dead adipocytes (24). We quantified CLSs in visceral and subcutaneous adipose tissue of WT and Plin2(Δ5) mice fed the HF diet for 12 weeks (**Fig. 6**). Significant numbers of CLSs were evident in epididymal (visceral) adipose tissue of WT mice (Fig. 6, panels A and D). We verified that these CLSs were composed of macrophages by F4/80 immunohistochemical staining (Fig. 6B). In agreement with previous studies (24), we found that CLS macrophages were enriched in Plin2-coated lipid droplets (Fig. 6C). In contrast, we did not detect significant numbers of CLSs in epididymal adipose tissue of HF-fed Plin2(Δ5) mice, or in subcutaneous adipose tissue of WT or Plin2(Δ5) mice (Fig. 6D). The reduction in CLSs is consistent with and perhaps explained by the reduced size of epididymal adipocytes observed in HF-fed Plin2(Δ5) mice.

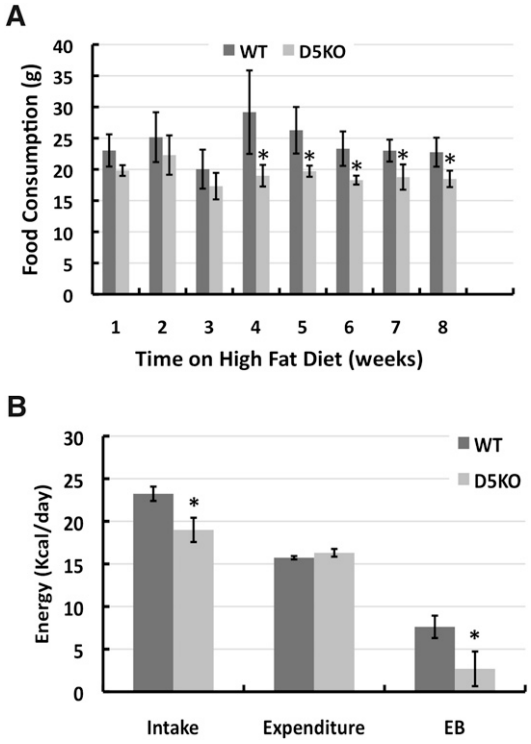

Fig. 4. Plin2 loss reduces food consumption and alters energetic properties. A: Weekly food consumption for male WT and Plin2(Δ5) mice fed the HF diet for 8 weeks. Food consumption values are average weights (g) of food consumed per week (± SD) for WT (N = 8) and Plin2(Δ5) (N = 8) mice. B: Energy intake (Intake), weight-adjusted energy expenditure (Expenditure), and energy balance (EB) values for male WT (N = 4) and Plin2(Δ5) (N = 4) mice on week 8 of HF feeding. The values are mean (± SD) for cohorts of four mice. Statistically significant differences are indicated by asterisks.

Plin2 loss prevents obesity-associated fatty liver disease

Nonalcoholic fatty liver disease is a common pathological feature of obesity in humans and in rodent models (25, 26). Because Plin2 deficiency has been reported to reduce lipid accumulation in livers of mice following 4 week exposure to a 45% fat diet (12, 13), we investigated whether our line of Plin2-null mice also prevented hepatic pathology associated with obesity in a prolonged feeding model. H and E staining of liver sections from WT and Plin2(Δ5) mice fed the HF diet for 12 weeks showed significant steatosis in livers of WT but not Plin2(Δ5) mice (**Fig. 7A**). In livers of WT mice, we observed a microvesicular pattern (vesicle diameter <10 μm) of steatosis in hepatocytes adjacent to the central vein (zone 3) and in the midlobular region (zone 2) (small arrow, Fig. 7A). In addition, we observed a macrovesicular pattern (vesicle diameter >10 μm) of steatosis in the peri-portal region (zone 1) (large arrow, Fig. 7A). However, this macrovesicular pattern was attenuated and not present in all hepatocytes. Consistent with this histological evidence, we found that total TG in Plin2(Δ5) livers was only about 10% of that found in WT livers (Fig. 7B) ($P < 0.001$), and that serum TG and FA levels were significantly lower ($P < 0.008$) in Plin2(Δ5) mice compared with WT mice (Table 1). The effects of a HF diet on liver pathology in WT and Plin2(Δ5) mice were categorized using the Kleiner/Brunt system as adapted to rodents (26) (Table 2). The results show that after 12 weeks on the HF diet, in addition to steatosis, WT mice exhibited a limited degree of additional liver pathology, predominantly microgranulomas, whereas evidence of inflammation and fatty liver disease was not detected in Plin2(Δ5) mice.

Plin2 deficiency in hepatocytes has been suggested to increase activation of peroxisome proliferator-activated receptor α (PPARα) (27). We quantified transcript levels of PPARα in livers of WT and Plin2(Δ5) mice fed HF or LF diets for 12 weeks (Fig. 7C). In animals on the LF diet, we found that hepatic PPARα transcript levels in Plin2(Δ5) mice were nearly 50% higher than those of WT mice

($P < 0.005$). Consistent with known stimulating effects of elevated FAs on PPARα expression (28), we found that there was a significant increase in PPARα transcript levels in 12 week HF-fed WT mice compared with mice on the LF diet ($P < 0.007$). However, PPARα transcript levels in 12 week HF-fed Plin2(Δ5) mice did not differ from those of LF-fed littermates or HF-fed WT mice. Elevated PPARγ expression is also thought to be a general property of fatty livers (29), and to possibly contribute to hepatic TG regulation (30). Consistent with the observation that Plin2(Δ5) mice on a HFD are protected against development of fatty liver, we found that hepatic PPARγ transcript levels of HF-fed Plin2(Δ5) mice were significantly ($P < 0.01$) less than those of WT mice (Fig. 7C). We did not detect differences in PPARγ transcript levels in livers of WT and Plin2(Δ5) mice fed the LF diet (Fig. 7C).

In addition to Plin2, Plin1 and Plin3 have been shown to coat hepatic CLDs in humans and mice under certain pathological conditions (25, 26), and there is evidence that Plin3 and -5 are capable of partially compensating for loss of Plin2 in stabilizing CLD accumulation in some cell types (31). To assess the possible roles of other PLIN family members in the hepatic responses to a chronic HF diet in WT and Plin2(Δ5) mice, and to determine if loss of Plin2 is associated with compensatory changes in other PLIN family members, we investigated the entire PLIN

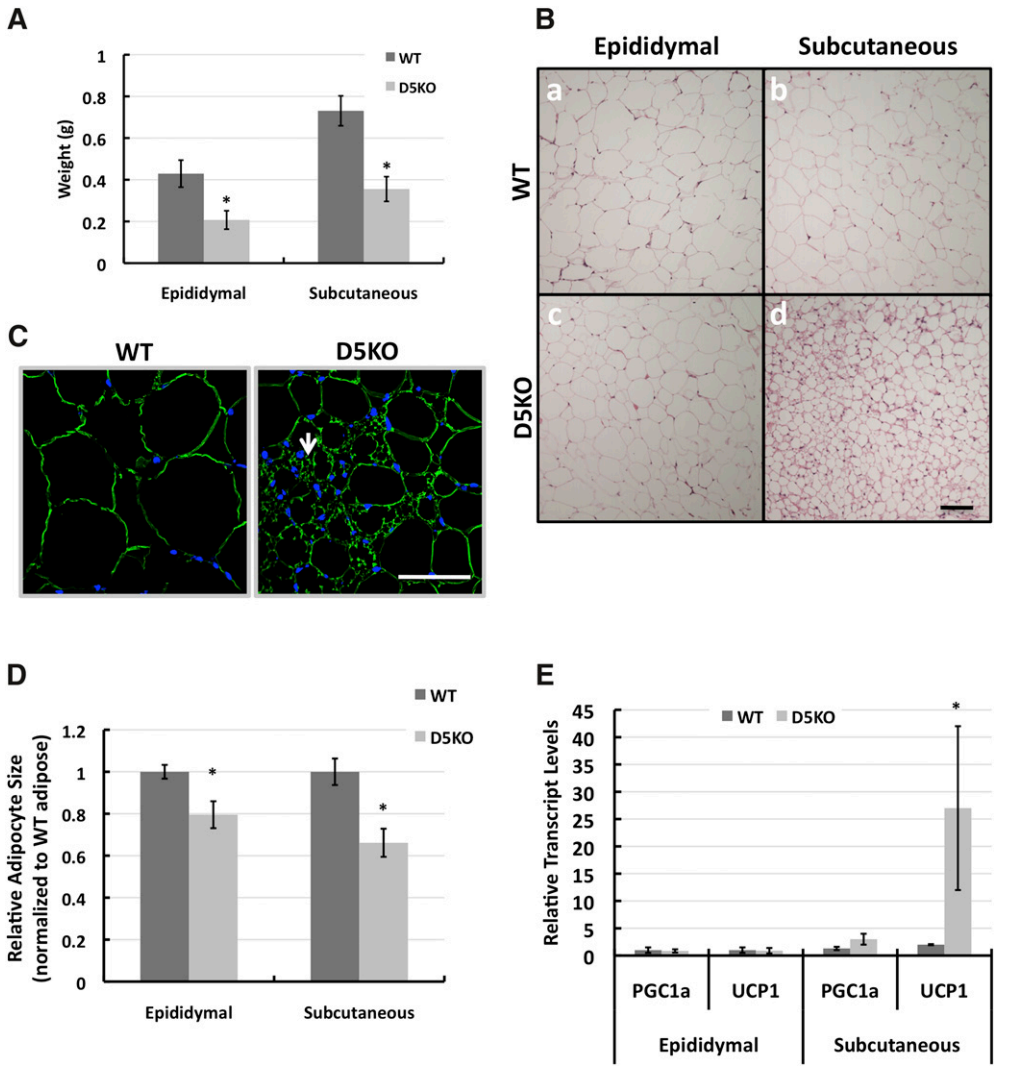

Fig. 5. Effects of Plin2 absence on adipose properties. A: Average (± SD) epididymal and subcutaneous adipose weights of male WT (N = 8) and Plin2(Δ5) (N = 8) mice on week 12 of HF feeding. B: Histology of adipocytes in epididymal (a, c) and subcutaneous (b, d) adipose tissue from male WT (a, b) and Plin2(Δ5) (c, d) mice on week 12 of HF feeding. Images show representative H and E-stained sections. C: Plin1 immunostaining of sections of subcutaneous adipose tissue from male WT and Plin2(Δ5) males on week 12 of HF feeding, showing the presence of adipocytes with multilocular droplets (arrow) in Plin2(Δ5) adipocytes. D: Relative adipocyte sizes of male WT and Plin2(Δ5) mice on week 12 of HF feeding. The values are shown relative to the average diameters of WT epididymal tissue and subcutaneous adipocytes (48 μm and 46 μm, respectively). E: Average (± SD) PGC1α and UCP1 transcript levels in epididymal and subcutaneous adipose tissue of WT (N = 4) and Plin2(Δ5) (N = 4) mice fed the HF diet for 9 weeks. Statistically significant differences are indicated by asterisks. Scale bars, 50 μm.

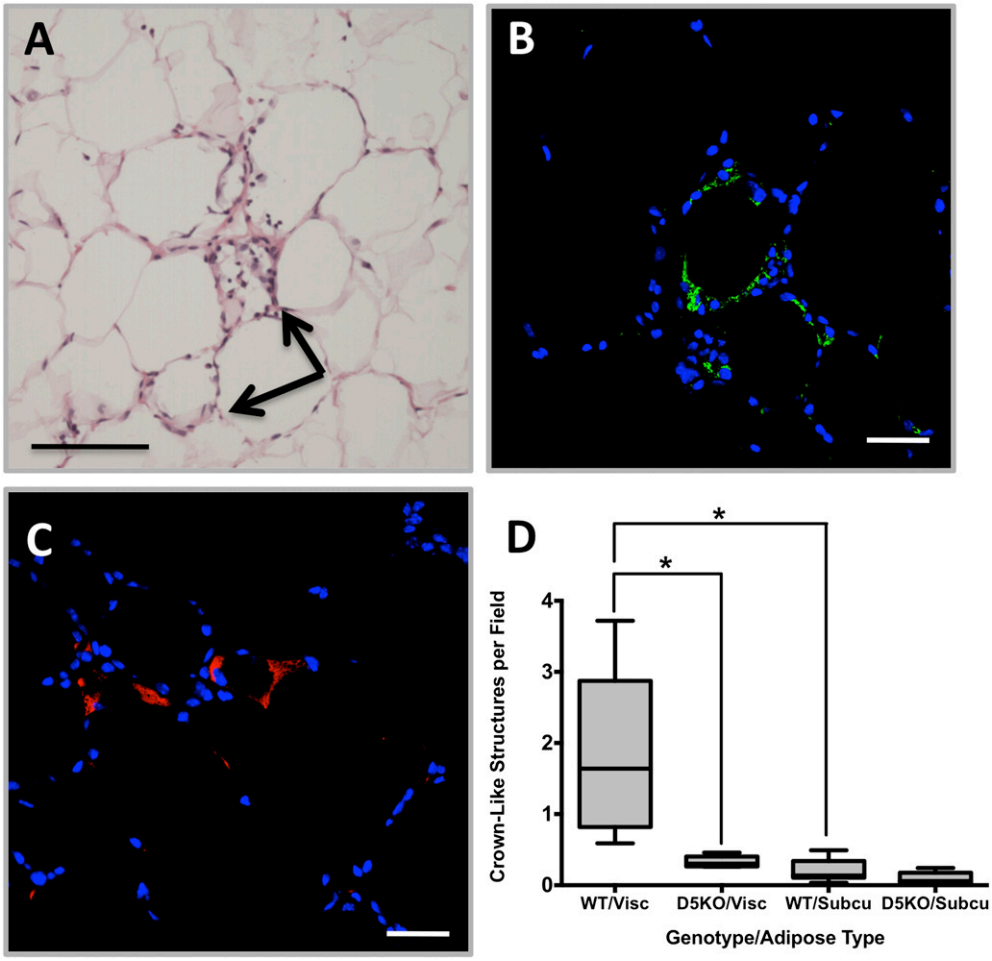

Fig. 6. Plin2 loss reduces inflammatory foci (crown-like structures) in visceral adipose. Representative visceral adipose sections from a male WT mouse fed the HF diet for 12 weeks stained with H and E (A) to identify CLSs, arrows in panel A. B: Immunostaining with F4/80 antibodies (green) documents the presence of macrophages in CLSs. C: Immunostaining with Plin2 antibodies (red) shows lipid droplet accumulation in cells of the CLS. D: Relative quantities (means ± SD) of CLSs in epdidiymal (Visc) and subcutaneous (Subcu) adipose tissue from WT (N = 8) and Plin2(Δ5) mice (N = 8). Statistically significant differences are indicated by asterisks. Scale bars: 50 μm (A), 20 μm (B, C).

family member expression profile. Figure 7D shows the relative transcript levels of PLIN family members in extracts of livers of these mice after HF or LF feeding for 12 weeks. We did not detect transcripts for Plin1 in liver extracts of WT or Plin2(Δ5) mice on either diet. Transcripts for Plins 2–5 were detected in livers of HF- and LF-fed WT mice; however, Plin2 transcript levels were 40–70 times greater than those of the other PLIN family members (Fig. 7D). Consistent with the known effects of HF feeding on Plin2 expression (32), we found that transcript levels of Plin2 in liver extracts of HF-fed WT mice were approximately twice those found in extracts of LF-fed mice ($P < 0.01$). However, transcript levels for Plins 3–5 were not affected by diet. Because the regulation of PLIN family member levels occurs by transcriptional and posttranscriptional mechanisms (33, 34), we next investigated by immunoblot analysis whether Plin2 loss affects other PLIN family member protein levels in livers of mice fed the HF diet for 12 weeks (Fig. 7E). We did not detect significant Plin1 or Plin4 immunoreactivity in extracts of livers from WT or Plin2(Δ5) mice (data not shown). Liver extracts from WT and Plin2(Δ5) mice on the HF diet had similar levels of Plin3, whereas Plin5 immunoreactivity was detected only in liver extracts of Plin2(Δ5) mice. Immunohistochemical staining of liver sections from 12 week HF-fed WT and Plin2(Δ5) mice demonstrated that hepatocyte CLDs in WT mice were selectively coated with Plin2 (Fig. 7F, panel a). In contrast, the few hepatocyte CLDs present in Plin2(Δ5) mice were selectively coated with Plin5 (Fig. 7F, panel j), whereas Plin3-coated CLDs were found in stellate cells located in the sinusoids (Fig. 7F, panel f). Interestingly, increased Plin5 levels are typically expressed in cells that have enhanced capacity for lipid oxidation (35, 36), and its expression is increased in Plin2(Δ5) livers. In summary, absence of Plin2 expression in liver protects against development of NAFLD in response to a HF diet and is associated with increased expression of Plin5.

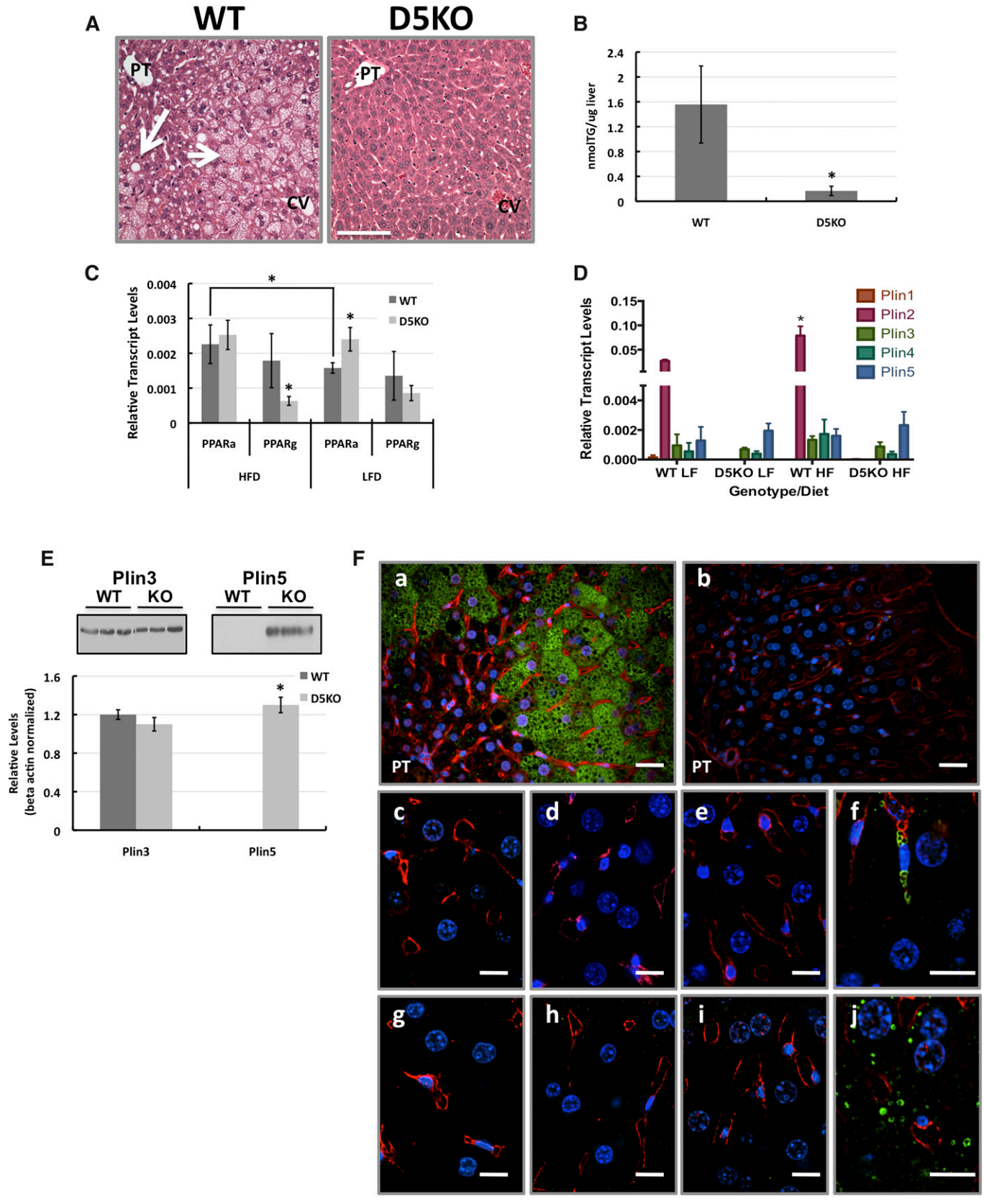

Fig. 7. Plin2 loss prevents obesity-associated fatty liver disease. A: Representative H and E-stained liver sections from male WT and Plin2(Δ5) mice fed the HF diet for 12 weeks. Areas of microsteatosis and macrosteatosis in sections from WT livers are indicated by short and long arrows, respectively. Histologically evident steatosis was not detected in livers of Plin2(Δ5) mice. PT, portal triad; CV, central vein. Scale bar, 100 μm. B: Hepatic triglyceride (TG) levels in WT (N = 8) and Plin2(Δ5) (N = 7) mice fed the HF diet for 12 weeks. Values are mean TG/mg liver (± SD). C: Hepatic PPARα (PPARa) and PPARγ (PPARg) transcript levels in WT and Plin2(Δ5) mice fed HF or LF diets

DISCUSSION

Our data provide several new insights into the physiological functions of Plin2 in mice. Utilizing a novel Plin2-null mouse model [Plin2(Δ5)], we demonstrate for the first time that Plin2 loss interferes with HF diet-induced obesity, and that the physiological basis of this effect appears, in part, to be related to reduced energy intake, and possibly to increased activity. Previous studies, using genetic or antisense models of Plin2 deficiency, failed to characterize effects of Plin2 loss on diet-induced obesity (12, 13). Our data suggest that this was not observed in these prior studies, in part due to insufficient time of exposure to HF diets, although in the case of the antisense model, it is possible that failure to detect HF diet-induced changes in body weight were also related to a more tissue restricted knockdown of Plin2. We found that differences in the weights of WT C57BL/6 mice and C57BL/6 mice lacking Plin2 were not statistically apparent until after about 4 weeks of HF diet feeding, which was the total length of time of HF diet exposure in the previous studies (12, 13). Significantly, we found that when exposed to HF diet feeding for 12 weeks, the Plin2(Δ2,3) mouse model of Chang et al. (12) was also resistant to diet-induced obesity. Mammary glands of lactating female Plin2(Δ2,3) mice have been shown to produce an N-terminal-truncated form of Plin2 (15). However, we did not detect Plin2 products in liver extracts of male Plin2(Δ2,3) mice using N- or C-terminal-specific antibodies (data not shown), which is consistent with original observations that nonlactating Plin2(Δ2,3) mice are deficient in Plin2 (12). Thus, there appears to be general agreement in the responses of Plin2(Δ2,3) and Plin2(Δ5) models to prolonged HF diet feeding, demonstrating in both models that loss of Plin2 impairs obesity development.

Effects of Plin2 deficiency on energy intake have not been identified previously. Our data indicate that differences in weight gains between WT and Plin2-null mice occur after about 4 weeks of HF diet feeding and correlate with decreased food consumption by Plin2-null animals. These findings suggest that decreases in energy intake related to loss of Plin2 may be an adaptive response to HF feeding. Reductions in food intake may also have been an important contributor in the observed reductions in serum TG and FAs in Plin2(Δ5) mice. The mechanism(s) by which Plin2 influences energy intake and activity are unclear as yet, and may involve multiple organ systems, given Plin2's ubiquitous tissue distribution. To address the underlying mechanisms and role of specific tissues in mediating the effects of Plin2 ablation on food intake and energy metabolism in future studies, we will generate mouse lines in which Plin2 is ablated in specific tissues.

Plin2 deficiency induced by treatment with Plin2 antisense oligonucleotides has been linked previously to decreased fat mass in HF-fed mice (13). However, the effects of Plin2 deficiency on adipose content have not been consistent; for instance, in the Plin2(Δ2,3) model, Plin2 loss did not appear to affect the content or properties of adipose tissue (12). However, in these studies, the authors did not examine subcutaneous adipose tissue in their line of Plin2-null mice. Our data demonstrate that compared with WT mice, both Plin2(Δ2,3) and Plin2(Δ5) mice exhibit a similar reduction in fat mass after 12 weeks of HF feeding. Thus, in three different models, Plin2 loss is associated with the curtailment of fat mass increases due to long-term HF feeding. Further, the correlation of Plin2 loss with the presence in subcutaneous adipose tissue of smaller adipocytes, multilocular CLDs, and elevated expression of UCP1 and PGC1α genes, suggests that Plin2 may play a role in regulating adipose metabolic properties, and possibly conversion of white to beige adipose tissue. Because we did not observe alterations in metabolic rate in our study, the effects of beige cells in subcutaneous adipose tissue on the physiology of Plin2 mice are unclear and will be explored in future studies. How Plin2 affects adipose properties remains to be defined. However, it is conceivable that Plin2 could act indirectly through effects on energy intake regulation and/or directly through regulation of adipose lipid packaging (21).

Macrophage infiltration to form inflammatory foci in adipose tissue is a key feature of obesity-related pathology in humans and rodents (24, 37). Our data showing that the number these foci is dramatically decreased in epididymal adipose tissue of Plin2-null animals compared with WT controls provide the first evidence implicating Plin2 in obesity-dependent adipose pathophysiology. Inflammatory foci formation is known to positively correlate with adipocyte size (38). The observation that Plin2 loss results in significant decreases in the size of adipocytes in both the epididymal and subcutaneous adipose tissue suggests that Plin2 expression may contribute to inflammatory foci formation through effects on epididymal adipocyte size.

NAFLD is another common pathological feature of obesity. Plin2 deficiency has been documented previously to reduce fatty liver associated with HF feeding (12, 13). Our data extend this finding to show that Plin2 loss completely prevents the hepatosteatosis and other aspects of fatty liver disease that occur with 12 weeks of HF feeding in WT mice. Loss of hepatic Plin2 was further shown to be associated with dramatic upregulation of Plin5 levels in

for 12 weeks. Values are means (± SD) normalized to 18S RNA. WT-HF (N = 8); WT-LF (N = 6); Plin2(Δ5)-HF (N = 7); Plin2(Δ5)-LF (N = 6). D: Transcript levels for PLIN family members in livers of male WT and Plin2(Δ5) mice fed LF or HF diets for 12 weeks. Values are means (± SD) normalized to 18S RNA. WT-HF (N = 8); WT-LF (N = 6); Plin2(Δ5)-HF (N = 7); Plin2(Δ5)-LF (N = 6). E: Immunoblot analysis of Plins 3 and 5 protein levels in livers of male WT and Plin2(Δ5) fed the HF diet for 12 weeks. The blots in the insets show results from three representative WT and Plin2(Δ5) animals. Average relative levels (± SD) of Plin3 and Plin5 are shown in the graph. F: Immunolocalization of PLIN family members (green staining) in livers of male WT (a, c, d, g, h) and Plin2(Δ5) (b, e, f, i, j) fed the HF diet for 12 weeks. Plin2 (a, b); Plin1 (c, e); Plin3 (d, f); Plin4 (g, i); Plin5 (h, j). Nuclei (blue) are stained with DAPI. PT, portal triad. Statistically significant differences are indicated by asterisks. Scale bars: 20 μm (a, b), 10 μm (c–j).

hepatocytes of HF-fed mice. Plin5 is most highly expressed in oxidative tissues such as skeletal muscle, and it was initially thought to promote fat oxidation (18, 36). However, more-recent data suggest that Plin5 protects mitochondria against the increased flux of FAs to mitochondria that leads to oxidative stress (39, 40). Thus, expression of Plin5 may act to maintain the physiology of the hepatocyte in response to increased trafficking of FAs to mitochondria. Plin3 has been implicated as a possible regulator of lipid droplet accumulation in the absence of Plin2 (31). Although loss of Plin3 is associated with a mild reduction in hepatosteatosis in mice (41), our data showing that Plin3 selectively localizes to lipid droplets in stellate cells, but not hepatocytes, in livers of Plin2-null mice suggest that its role in hepatosteatosis may not be directly related to hepatocyte functions.

In summary, we document in two genetic mouse models that Plin2 loss attenuates diet-induced obesity, and further, we demonstrate that loss of Plin2 prevents obesity-associated adipose and hepatic pathological changes in mice. Although additional studies are needed to establish the physiological mechanisms underlying the effects of Plin2 on obesity, our data suggest that Plin2 plays an important role in energy homeostasis. We observed that normal Plin2 expression in the C57BL/6 line is critical to the obesity-prone phenotype that manifests with HF feeding. The loss of Plin2 yields an obesity-resistant phenotype characterized by adaptations in food intake and physical activity in response to this chronic dietary challenge. The gradual and integrative nature of this response may explain why Plin2 loss did not affect weight gains during shorter exposures to the HF diet (12, 13) or why Plin2 loss does not affect body weights of mice in which leptin receptor signaling is disrupted (42). Understanding how Plin2 is involved in the homeostatic control of energy balance will provide new insights into the mechanisms by which nutrition overload is detected and how individuals adapt to, or fail to adapt to, dietary challenges.

The authors thank Storey Wilson and the Prostrate Cancer Program for assistance with image analysis of adipose tissue, and acknowledge services provided by the Adipose Biology Core of the Colorado Obesity Research Initiative.

REFERENCES

1. Catenacci, V. A., J. O. Hill, and H. R. Wyatt. 2009. The obesity epidemic. *Clin. Chest Med.* **30:** 415–444.
2. Unger, R. H., G. O. Clark, P. E. Scherer, and L. Orci. 2010. Lipid homeostasis, lipotoxicity and the metabolic syndrome. *Biochim. Biophys. Acta.* **1801:** 209–214.
3. Fabbrini, E., F. Magkos, B. S. Mohammed, T. Pietka, N. A. Abumrad, B. W. Patterson, A. Okunade, and S. Klein. 2009. Intrahepatic fat, not visceral fat, is linked with metabolic complications of obesity. *Proc. Natl. Acad. Sci. USA.* **106:** 15430–15435.
4. Torres, D. M., and S. A. Harrison. 2012. Nonalcoholic steatohepatitis and noncirrhotic hepatocellular carcinoma: fertile soil. *Semin. Liver Dis.* **32:** 30–38.
5. Wang, Y., L. M. Ausman, A. S. Greenberg, R. M. Russell, and X. D. Wang. 2009. Nonalcoholic steatohepatitis induced by a high-fat diet promotes diethylnitrosamine-initiated early hepatocarcinogenesis in rats. *Int. J. Cancer.* **124:** 540–546.
6. Murphy, S., S. Martin, and R. G. Parton. 2009. Lipid droplet-organelle interactions; sharing the fats. *Biochim. Biophys. Acta.* **1791:** 441–447.
7. Greenberg, A. S., R. A. Coleman, F. B. Kraemer, J. L. McManaman, M. S. Obin, V. Puri, Q. W. Yan, H. Miyoshi, and D. G. Mashek. 2011. The role of lipid droplets in metabolic disease in rodents and humans. *J. Clin. Invest.* **121:** 2102–2110.
8. Brasaemle, D. L. 2007. The perilipin family of structural lipid droplet proteins: stabilization of lipid droplets and control of lipolysis. *J. Lipid Res.* **48:** 2547–2549.
9. Martinez-Botas, J., J. B. Anderson, D. Tessier, A. Lapillonne, B. H. Chang, M. J. Quast, D. Gorenstein, K. H. Chen, and L. Chan. 2000. Absence of perilipin results in leanness and reverses obesity in Lepr(db/db) mice. *Nat. Genet.* **26:** 474–479.
10. Tansey, J. T., C. Sztalryd, J. Gruia-Gray, D. L. Roush, J. V. Zee, O. Gavrilova, M. L. Reitman, C. X. Deng, C. Li, A. R. Kimmel, et al. 2001. Perilipin ablation results in a lean mouse with aberrant adipocyte lipolysis, enhanced leptin production, and resistance to diet-induced obesity. *Proc. Natl. Acad. Sci. USA.* **98:** 6494–6499.
11. Souza, S. C., L. M. de Vargas, M. T. Yamamoto, P. Lien, M. D. Franciosa, L. G. Moss, and A. S. Greenberg. 1998. Overexpression of perilipin A and B blocks the ability of tumor necrosis factor alpha to increase lipolysis in 3T3-L1 adipocytes. *J. Biol. Chem.* **273:** 24665–24669.
12. Chang, B. H., L. Li, A. Paul, S. Taniguchi, V. Nannegari, W. C. Heird, and L. Chan. 2006. Protection against fatty liver but normal adipogenesis in mice lacking adipose differentiation-related protein. *Mol. Cell. Biol.* **26:** 1063–1076.
13. Imai, Y., G. M. Varela, M. B. Jackson, M. J. Graham, R. M. Crooke, and R. S. Ahima. 2007. Reduction of hepatosteatosis and lipid levels by an adipose differentiation-related protein antisense oligonucleotide. *Gastroenterology.* **132:** 1947–1954.
14. Varela, G. M., D. A. Antwi, R. Dhir, X. Yin, N. S. Singhal, M. J. Graham, R. M. Crooke, and R. S. Ahima. 2008. Inhibition of ADRP prevents diet-induced insulin resistance. *Am. J. Physiol. Gastrointest. Liver Physiol.* **295:** G621–G628.
15. Russell, T. D., C. A. Palmer, D. J. Orlicky, E. S. Bales, B. H. Chang, L. Chan, and J. L. McManaman. 2008. Mammary glands of adipophilin-null mice produce an amino-terminally truncated form of adipophilin that mediates milk lipid droplet formation and secretion. *J. Lipid Res.* **49:** 206–216.
16. Wahlig, J. L., E. S. Bales, M. R. Jackman, G. C. Johnson, J. L. McManaman, and P. S. Maclean. 2012. Impact of high-fat diet and obesity on energy balance and fuel utilization during the metabolic challenge of lactation. *Obesity (Silver Spring)* **20:** 65–75.
17. Russell, T. D., C. A. Palmer, D. J. Orlicky, A. Fischer, M. C. Rudolph, M. C. Neville, and J. L. McManaman. 2007. Cytoplasmic lipid droplet accumulation in developing mammary epithelial cells: roles of adipophilin and lipid metabolism. *J. Lipid Res.* **48:** 1463–1475.
18. Dalen, K. T., S. M. Ulven, B. M. Arntsen, K. Solaas, and H. I. Nebb. 2006. PPARalpha activators and fasting induce the expression of adipose differentiation-related protein in liver. *J. Lipid Res.* **47:** 931–943.
19. Russell, T. D., J. Schaack, D. J. Orlicky, C. Palmer, B. H. Chang, L. Chan, and J. L. McManaman. 2011. Adipophilin regulates maturation of cytoplasmic lipid droplets and alveolae in differentiating mammary glands. *J. Cell Sci.* **124:** 3247–3253.
20. Brasaemle, D. L., T. Barber, N. E. Wolins, G. Serrero, E. J. Blanchette-Mackie, and C. Londos. 1997. Adipose differentiation-related protein is an ubiquitously expressed lipid storage droplet-associated protein. *J. Lipid Res.* **38:** 2249–2263.
21. Wolins, N. E., D. L. Brasaemle, and P. E. Bickel. 2006. A proposed model of fat packaging by exchangeable lipid droplet proteins. *FEBS Lett.* **580:** 5484–5491.
22. Ishibashi, J., and P. Seale. 2010. Medicine. Beige can be slimming. *Science.* **328:** 1113–1114.
23. Wu, Z., P. Puigserver, U. Andersson, C. Zhang, G. Adelmant, V. Mootha, A. Troy, S. Cinti, B. Lowell, R. C. Scarpulla, et al. 1999. Mechanisms controlling mitochondrial biogenesis and respiration through the thermogenic coactivator PGC-1. *Cell.* **98:** 115–124.
24. Cinti, S., G. Mitchell, G. Barbatelli, I. Murano, E. Ceresi, E. Faloia, S. Wang, M. Fortier, A. S. Greenberg, and M. S. Obin. 2005. Adipocyte death defines macrophage localization and function in adipose tissue of obese mice and humans. *J. Lipid Res.* **46:** 2347–2355.
25. Straub, B. K., P. Stoeffel, H. Heid, R. Zimbelmann, and P. Schirmacher. 2008. Differential pattern of lipid droplet-associated proteins and de novo perilipin expression in hepatocyte steatogenesis. *Hepatology.* **47:** 1936–1946.

26. Orlicky, D. J., J. R. Roede, E. Bales, C. Greenwood, A. Greenberg, D. Petersen, and J. L. McManaman. 2011. Chronic ethanol consumption in mice alters hepatocyte lipid droplet properties. *Alcohol. Clin. Exp. Res.* **35:** 1020–1033.
27. Sapiro, J. M., M. T. Mashek, A. S. Greenberg, and D. G. Mashek. 2009. Hepatic triacylglycerol hydrolysis regulates peroxisome proliferator-activated receptor alpha activity. *J. Lipid Res.* **50:** 1621–1629.
28. Issemann, I., R. A. Prince, J. D. Tugwood, and S. Green. 1993. The peroxisome proliferator-activated receptor:retinoid X receptor heterodimer is activated by fatty acids and fibrate hypolipidaemic drugs. *J. Mol. Endocrinol.* **11:** 37–47.
29. Moran-Salvador, E., M. Lopez-Parra, V. Garcia-Alonso, E. Titos, M. Martinez-Clemente, A. Gonzalez-Periz, C. Lopez-Vicario, Y. Barak, V. Arroyo, and J. Claria. 2011. Role for PPARgamma in obesity-induced hepatic steatosis as determined by hepatocyte- and macrophage-specific conditional knockouts. *FASEB J.* **25:** 2538–2550.
30. Gavrilova, O., M. Haluzik, K. Matsusue, J. J. Cutson, L. Johnson, K. R. Dietz, C. J. Nicol, C. Vinson, F. J. Gonzalez, and M. L. Reitman. 2003. Liver peroxisome proliferator-activated receptor gamma contributes to hepatic steatosis, triglyceride clearance, and regulation of body fat mass. *J. Biol. Chem.* **278:** 34268–34276.
31. Sztalryd, C., M. Bell, X. Lu, P. Mertz, S. Hickenbottom, B. H. Chang, L. Chan, A. R. Kimmel, and C. Londos. 2006. Functional compensation for adipose differentiation-related protein (ADFP) by TIP47 in an ADFP null embryonic cell line. *J. Biol. Chem.* **281:** 34341–34348.
32. Motomura, W., M. Inoue, T. Ohtake, N. Takahashi, M. Nagamine, S. Tanno, Y. Kohgo, and T. Okumura. 2006. Up-regulation of ADRP in fatty liver in human and liver steatosis in mice fed with high fat diet. *Biochem. Biophys. Res. Commun.* **340:** 1111–1118.
33. Bickel, P. E., J. T. Tansey, and M. A. Welte. 2009. PAT proteins, an ancient family of lipid droplet proteins that regulate cellular lipid stores. *Biochim. Biophys. Acta.* **1791:** 419–440.
34. Hall, A. M., E. M. Brunt, Z. Chen, N. Viswakarma, J. K. Reddy, N. E. Wolins, and B. N. Finck. 2010. Dynamic and differential regulation of proteins that coat lipid droplets in fatty liver dystrophic mice. *J. Lipid Res.* **51:** 554–563.
35. Bosma, M., R. Minnaard, L. M. Sparks, G. Schaart, M. Losen, M. H. de Baets, H. Duimel, S. Kersten, P. E. Bickel, P. Schrauwen, et al. 2012. The lipid droplet coat protein perilipin 5 also localizes to muscle mitochondria. *Histochem. Cell Biol.* **137:** 205–216.
36. Wolins, N. E., B. K. Quaynor, J. R. Skinner, A. Tzekov, M. A. Croce, M. C. Gropler, V. Varma, A. Yao-Borengasser, N. Rasouli, P. A. Kern, et al. 2006. OXPAT/PAT-1 is a PPAR-induced lipid droplet protein that promotes fatty acid utilization. *Diabetes.* **55:** 3418–3428.
37. Strissel, K. J., Z. Stancheva, H. Miyoshi, J. W. Perfield II, J. Defuria, Z. Jick, A. S. Greenberg, and M. S. Obin. 2007. Adipocyte death, adipose tissue remodeling, and obesity complications. *Diabetes.* 56: 2910–2918.
38. Weisberg, S. P., D. McCann, M. Desai, M. Rosenbaum, R. L. Leibel, and A. W. Ferrante, Jr. 2003. Obesity is associated with macrophage accumulation in adipose tissue. *J. Clin. Invest.* **112:** 1796–1808.
39. Wang, H., U. Sreenevasan, H. Hu, A. Saladino, B. M. Polster, L. M. Lund, D. W. Gong, W. C. Stanley, and C. Sztalryd. 2011. Perilipin 5, a lipid droplet-associated protein, provides physical and metabolic linkage to mitochondria. *J. Lipid Res.* **52:** 2159–2168.
40. Kuramoto, K., T. Okamura, T. Yamaguchi, T. Y. Nakamura, S. Wakabayashi, H. Morinaga, M. Nomura, T. Yanase, K. Otsu, N. Usuda, et al. 2012. Perilipin 5, a lipid droplet-binding protein, protects heart from oxidative burden by sequestering fatty acid from excessive oxidation. *J. Biol. Chem.* **287:** 23852–23863.
41. Carr, R. M., R. T. Patel, V. Rao, R. Dhir, M. J. Graham, R. M. Crooke, and R. S. Ahima. 2012. Reduction of TIP47 improves hepatic steatosis and glucose homeostasis in mice. *Am. J. Physiol. Regul. Integr. Comp. Physiol.* **302:** R996–R1003.
42. Chang, B. H., L. Li, P. Saha, and L. Chan. 2010. Absence of adipose differentiation related protein upregulates hepatic VLDL secretion, relieves hepatosteatosis, and improves whole body insulin resistance in leptin-deficient mice. *J. Lipid Res.* **51:** 2132–2142.